Journal of Power Sources 196 (2011) 6153–6159

Contents lists available at ScienceDirect

Journal of Power Sources

journal homepage: www.elsevier.com/locate/jpowsour

In and ex situ characterization of an anion-exchange membrane for alkaline direct methanol fuel cell (ADMFC)

Annukka Santasalo-Aarnio[a], Sami Hietala[b], Taina Rauhala[a], Tanja Kallio[a,*]

[a] Research group of Fuel Cells, Department of Chemistry, Aalto University, P.O. Box 16100, 00076 Aalto, Finland
[b] Laboratory of Polymer Chemistry, Department of Chemistry, University of Helsinki, P.O. Box 55, FIN-00014 HU, Finland

ARTICLE INFO

Article history:
Received 4 November 2010
Received in revised form 8 March 2011
Accepted 12 March 2011
Available online 22 March 2011

Keywords:
Anion exchange membrane (AEM)
Alkaline direct methanol fuel cell (ADMFC)
Conductivity
Methanol crossover
Differential scanning calorimetry (DSC)
Electrochemical impedance spectroscopy (EIS)

ABSTRACT

Anion exchange membrane fumasep® FAA-2 was characterized with ex and in situ methods in order to estimate the membranes' suitability as an electrolyte for an alkaline direct methanol fuel cell (ADMFC). The interactions of this membrane with water, hydroxyl ions and methanol were studied with both calorimetry and NMR and compared with the widely used proton exchange membrane Nafion® 115. The results indicate that FAA-2 has a tighter structure and more homogeneous distribution of ionic groups in contrast to the clustered structure of Nafion, moreover, the diffusion of OH^- ions through this membrane is clearly slower compared to water molecules. The permeability of methanol through the FAA-2 membrane was found to be an order of magnitude lower than for Nafion. Fuel cell experiments in 1 mol dm^{-3} methanol with FAA-2 resulted in OCV of 0.58 V and maximum power density of 0.32 mW cm^{-2}. However, even higher current densities were obtained with highly concentrated fuels. This implies that less water is needed for fuel dilution, thereby decreasing the mass of the fuel cell system. In addition, electrochemical impedance spectroscopy for the ADMFC was used to determine ohmic resistance of the cell facilitating the further membrane development.

1. Introduction

Polymer electrolyte fuel cells (PEFCs) have been studied intensively for decades; however, commercial breakthrough has not been attained due to the expensive cell components such as the catalyst materials and the membrane used as an electrolyte. For low power demand applications, such as laptops, methanol is an interesting fuel thanks to its high energy density and easy storability compared to hydrogen gas. When this alcohol is used as a fuel for PEFCs the cell is called direct methanol fuel cell (DMFC). In this type of fuel cells methanol is oxidized at the anode to electrons and protons which are transported through the proton exchange membrane (PEM) to the cathode. The formation and release of these protons lowers the pH on both sides of the membrane electrode assembly (MEA). Unfortunately, in acidic media methanol oxidation is sluggish resulting in low power densities even with high loadings of noble metal catalysts. In contrast, electrode reactions are enhanced in alkaline media [1] and therefore, the amount of catalyst material can be reduced. With high pH also non noble metal catalysts can be used for both the electrode reactions, methanol oxidation [2–5] and oxygen reduction [6–8], even at low temperatures. In spite of these advantages, alkaline DMFCs have not been widely studied due to the lack of anion (hydroxyl ion) exchange membranes (AEM) that are durable during fuel cell test. These kinds of materials have only recently been introduced [9–16].

Polymeric AEM materials contain covalently bonded positive ionic groups such as quaternary ammonium (QA) functional groups (poly-N^+Me_3) which attract negatively charged OH^- or Cl^- ions [17]. The mobility of these large anions is slower than that of small H^+ [18] resulting in lower conductivity compared to acidic PEMs. The hydroxyl ions create locally a high pH around the catalyst particles changing the reaction mechanisms on both electrodes whereas the total cell reaction remains identical to the one in the conventional PEM DMFC:

$$\text{Anode}: \ CH_3OH + 6OH^- \rightarrow CO_2 + 5H_2O + 6e^- \quad \text{(i)}$$

$$\text{Cathode}: \ 3/2O_2 + 3H_2O + 6e^- \rightarrow 6OH^- \quad \text{(ii)}$$

$$\text{Total}: \ CH_3OH + 3/2O_2 \rightarrow CO_2 + 2H_2O \quad \text{(iii)}$$

The advantages of these materials compared to the conventional PEM have been listed in previous studies; AEMs typically have lower methanol permeability due to the dense membrane structure and the ion transport from the cathode to anode that is reverse to methanol crossover [9,16]. As a result mixed potentials decrease on the cathode increasing the open circuit potential of the whole cell. With less severe crossover, thinner electrolytes can be used

* Corresponding author. Tel.: +358 9470 22583; fax: +358 9470 22580.
E-mail address: tanja.kallio@tkk.fi (T. Kallio).

0378-7753/$ – see front matter © 2011 Elsevier B.V. All rights reserved.
doi:10.1016/j.jpowsour.2011.03.028

reducing the total resistance of the cell. In addition, water is produced at the anode side and consumed at the cathode (Reactions (i) and (ii)) facilitating the water management of the cell [19].

The main drawback of AEMs is the ion conductivity, which is still almost ten times lower than that for PEMs, clearly limiting the current densities obtained from the fuel cell [9–16]. To increase the current density of the alkaline DMFC several groups have used mixtures of alcohol with diluted NaOH or KOH (pH 14) solutions as anode fuels [9–15]. These experiments demonstrate that with further development of the conductivity properties of AEM materials the current densities obtained can compete with the ones obtained from the PEM DMFC. However, in real applications the use of high pH fuel would not be a viable option due to the rapid component corrosion and carbonation of the anode fuel.

Previous publications have reported mainly ex situ properties of the new AEM materials and the only in situ results presented have been polarization curves. However, another in situ method, electrochemical impedance spectroscopy (EIS), could complete the analysis by giving more detailed information on the different phenomena occurring in the cell. This method has previously only been used for studying AEMs in the hydrogen PEFCs where the electrode kinetics differ from those in the alkaline DMFC and therefore the same models do not apply.

This work presents selected ex situ physical properties of a new anion exchange membrane fumasep® FAA-2 by Fumatech, as a function of methanol concentration and compare them with the commercial Nafion® 115 membrane. In addition, MEAs with this AEM were successfully prepared and in situ alkaline DMFC performance and impedance are presented at different methanol concentrations. Finally, a corresponding equivalent circuit for the alkaline DMFC is presented and compared with the experimental data.

2. Experimental

2.1. Ex situ membrane characterization

New commercial fumasep® FAA-2 membrane provided by Fumatech Company was selected as the AEM due to the required mechanical stability and ease of use during the MEA preparation procedure. The ion exchange capacity provided by the manufacturer for this membrane is 1.39 meq g^{-1} and thickness for dry membrane between 55 and 65 μm. The membrane was obtained in Cl^- form and exchanged to OH^- form by equilibration in 0.5 mol dm^{-3} NaOH (Merck, p.a.) for several days prior to membrane characterization. For crossover experiments and fuel cell MEA preparation the membrane was ion exchanged at room temperature with 0.5 mol dm^{-3} KOH (J.T. Baker p.a.) solution for 24 h with stirring, followed by stabilizing in Milli-Q water (MQ, 0.04 μS cm^{-1}, Millipore) for 24 h. Nafion 115® membrane (Du Pont) was used as a reference material and pretreated by boiling in 5% H_2O_2 for 30 min followed by careful rinsing with MQ-water and boiling for 30 min in MQ-water. After this the membrane was boiled in 0.5 mol dm^{-3} H_2SO_4 in order to exchange it to the protonated form, followed by rinsing and boiling several times with MQ-water.

To measure the liquid uptake from water–methanol solutions, samples were soaked in solutions and left to equilibrate at room temperature for at least 48 h. Excess liquid was removed by blotting the surface. Samples were weighed immediately and the ratio of the mass of the absorbed solvent to the mass of the dry sample (dried over P_2O_5 for 10 days) was calculated and expressed as liquid uptake (g g^{-1}) of dry membrane. Sorption and desorption of water were followed by placing membrane samples in a closed vessel containing a saturated salt solution corresponding to different relative humidities [20] and leaving them to equilibrate for at least 7 days (preliminary tests showed that this was sufficient for equilibrium to be reached). The samples were then weighed and placed to equilibrate over the next solution. At least 5 parallel membrane samples were measured and the average of these values is presented. Measuring the masses of samples equilibrated with concentrated methanol solution was less repeatable due to the volatile nature of these solutions.

Normal conductivities of the membranes in different aqueous methanol solutions were recorded by impedance spectroscopy [21,22]. The membranes were pressed with 20 bar force between two platinum disks with a diameter of 5 mm. The electrodes were connected to an Autolab PGSTAT 20 potentiostat supplied with a FRA 4.9 software. Prior to these measurements membranes were equilibrated in the same manner as in the case of liquid uptake measurements described above. The spectra were recorded using frequency range from 1 to 900 kHz and the resistance was determined by extrapolating the linear part and/or the semi-circle to the real axis. The conductivity was calculated from the resistance using the electrode area and membrane thickness, the latter measured with a micrometer.

Thermal decomposition of dried membrane samples was studied with thermogravimetry (TGA) at 25–800 °C using heating rate of 10 °C min^{-1} under flowing nitrogen atmosphere with Mettler-Toledo TGA850. Differential scanning calorimetry (DSC) measurements were performed with a Mettler 822e DSC under nitrogen atmosphere. Membranes immersed into different water–methanol solutions for one week were gently wiped with paper tissue and hermetically sealed in aluminum pans. For calorimetric measurement the samples were first cooled from room temperature to −160 °C for 10 min and then heated up to 30 °C at 10 °C min^{-1}. The melting of water contained in the membranes was identified by integration of the heat absorptions. The enthalpy change was normalized to the melting of water by subtracting the weight of dry membrane and methanol in the mixture. The amount of freezable water was calculated using the heat of fusion of pure water, 334 J g^{-1} [23] and assuming that the solvent composition in the membrane was the same as that of the binary liquid in which it had been immersed [24].

For the NMR measurements, the boiled membrane samples were immersed in perdeuterated water (D_2O)/methanol (CD_3OD) mixtures of known composition for a period of a few days or, to obtain membrane at 100% relative humidity, placed in saturated D_2O environment. Perdeuterated methanol was used to avoid signal saturation problems. Proton NMR spectra and pulsed field gradient (PFG–NMR) diffusion experiments were carried out with a Varian UNITYINOVA spectrometer operating at 300 MHz for protons. For the diffusion measurements, the temperature was set at 22 °C and a stimulated echo sequence with a gradient pulse σ duration of 2 ms and a dwell time Δ = 20 ms between the first and last 90° pulse was applied. Thirty spectra were recorded over linearly incremented gradient strengths of 0–65 G cm^{-1}. The diffusion coefficients for signals arising from bound water at 4.6 ppm were calculated from the slope of the signal intensities versus gradient strength, obtained with a regression fit of the raw data. The instrument was calibrated by measuring the diffusion coefficient of a water sample under the same experimental conditions, and the spectra were referenced according to the external water peak at 4.8 ppm. The diffusion coefficient of hydroxyls in the membrane has been obtained with Nernst–Einstein equation:

$$D_i = RTu_i = RT\frac{\kappa_i}{c_i z_i^2 F^2} \quad (1)$$

where u_i is mobility, κ_i conductivity and c_i concentration of the hydroxyl ion in the membrane, R is gas constant and T temperature.

Methanol crossover experiments were performed in a diffusion cell with two glass compartments (volume of each 3 ml). The

studied membrane was moistened with MQ-water for 24 h prior to the experiments and then placed between the cells. One of the compartments was then filled with water–methanol solution and simultaneously the other with MQ-water. Both compartments had magnetic stirrers to ensure that no concentration gradients were formed and the temperatures of the solutions inside were stabilized with water circulation to 30 ± 0.5 °C. Samples of 30 μl were taken from the water side at various times and 10 μl of 1 mol dm^{-3} 1,4-dioxine was added to each sample as an internal standard. The samples were analyzed with a gas chromatograph (HP 6890 GC) using a HP-innowax column at heating rate of 4 °C min^{-1} and a FID detector. The methanol permeability through the membrane has been calculated with the model of linear time concentration correspondence used in several studies for fuel cell membranes [16,25,26]. The model is fitted to the first 60 min of the experimental data and the methanol permeability is estimated by

$$c_m = \frac{APc_m^0}{Vl}\left(t - \frac{l^2}{6D_m}\right) \quad (2)$$

where A is area of the membrane exposed to crossover (0.673 cm^2), c_m^0 initial concentration of methanol at the chamber, V volume of the chambers (3 ml), l membrane thickness measured after the crossover experiment and P permeability coefficient expressed as

$$P = D_m K \quad (3)$$

where D_m is diffusion coefficient of methanol and K partition coefficient.

2.2. MEA preparation

Prior to the fuel cell experiments a membrane electrode assembly (MEA) with the studied anion exchange membrane was prepared. The catalyst ink was prepared by mixing catalyst (Pt on Vulcan for the cathode and PtRu on Vulcan for the anode, both having loading of 1 mg cm^{-2} and supplied by Alfa Aesar), alkaline ionomer (similar to membrane material) and 2-propanol as a solvent. The inks were first stirred with a magnetic stirrer for an hour and after that with an ultrasonicator. The slurry was painted onto the membrane materials with an air brush and the assembly dried in a vacuum oven for 2 h. After both the electrodes were painted onto the membrane, the MEA was heat pressed at 80 °C, with 1 metric tons pressure for 80 s. A fuel cell from Fuel Cell Technologies was assembled with the MEA, Teflon gaskets and gas diffusion layers (carbon cloth with 10% (anode) or 60% (cathode) Teflon), after which the cell was closed and tightened evenly with a torque of 10 kN.

2.3. In situ membrane characterization

The fuel cell experiments were performed in a single cell with a surface area of 7.29 cm^2. The liquid fuel (prepared from methanol (Merck, p.a.) and MQ-water) was fed to the anode with a rate of 2 ml min^{-1} and dried oxygen gas (Aga, purity 99.999%) to the cathode at 300 ml min^{-1}. The temperature of the cell was controlled to be 30 °C ± 1 °C. The cell was stabilized overnight with the studied methanol fuel at a flow rate of 0.2 ml min^{-1} and oxygen with 30 ml min^{-1} and normalized 2 h prior to the experiments with higher feed rates. The polarization curves were measured with a PGSTAT 20 instrument equipped with an Ecochemie 10 A current booster BSTR10A and GPES software starting from the OCV linearly to 0.05 V at the rate of 0.5 mV s^{-1}. Impedance was recorded from the cell with the same instrumentation as in the case of the conductivity measurements. The spectra were recorded galvanostatically to ensure that the reaction rate remained the same during the whole experiment. The frequencies studied were between 0.01 Hz and 100 kHz and the amplitude 5% of the current applied. The data obtained was analysed with the Z-view 2.3d application.

Table 1
Thickness, liquid uptake and conductivity of the studied membrane materials.

cMeOH (mol l^{-1})	Thickness wet (μm)	Liquid uptake (g g^{-1} dry polymer)	Conductivity (mS cm^{-1})
FuMA-Tech FAA-2			
0	25	1.0	0.92
1	30	1.6	3.26
5	37	1.8	2.74
10	42	1.0	1.00
15	47	0.9	0.94
24.75	50	1.0	–
Nafion 115			
0	143	0.36	54
1	145	0.37	47
5	150	0.66	44
10	155	0.67	40
15	160	0.69	31
24.75	160	0.89	23

3. Results and discussion

3.1. Ex situ membrane properties

Selected properties of the membrane characterization are presented in Table 1. At all methanol concentrations the FAA-2 AEM is at least 3 times thinner compared to Nafion 115. Nevertheless, the former swells with increasing methanol concentration and doubles its thickness in pure methanol solution. The initially thicker Nafion 115 membrane has a thickness increase of 12% in pure methanol compared to that in water. The liquid uptake of the FAA-2 membrane increases with the low methanol concentration until 5 mol dm^{-3} (Table 1) which correlates with the changes in the membrane thickness. However, with higher concentrations, the liquid uptake values decrease back to the level of pure water even though the membrane thicknesses continue increasing. This phenomenon would indicate that with concentrated methanol solution some kind of a structural change is occurring in the membrane matrix. For the Nafion 115 membrane the liquid uptake is lower and it increases linearly with methanol concentration along with the membrane thickness.

The normal conductivities of both the membranes decreases when more methanol is present, however, for FAA-2 the conductivity in pure water is lower than in any methanol solution. This also indicates that in the presence of methanol structural changes occur in the AEM which needs to be identified in further studies. The conductivities presented in Table 1 for FAA-2 are of the same order as values reported for other AEM materials at low temperatures [27–29]. These values are almost a decade lower than the corresponding values for Nafion 115 reflecting the differences in the structure of the membranes and the mobility of OH^- and H^+ ions [18]. Nevertheless, conductivity depends also on the membrane thickness according to the measurement method: when normal conductivities are measured the value increases with membrane thickness [30]. Silva et al [30] have obtained normal conductivities of 33 and 23 mS cm^{-1} that corresponds wet membrane thicknesses of 149 and 55 μm for Nafion® 115 and 112, respectively. This indicates that if one would have Nafion material with similar thickness than FAA-2 the expected conductivity would be even lower than what obtained with Nafion 112. Overall, it is worth keeping mind that the development of AEM materials for this purpose has been ongoing only for a short time and the conductivities of these materials can be further optimized.

In order to understand the properties, especially ion transport, of the new membrane material, physical characterization has been

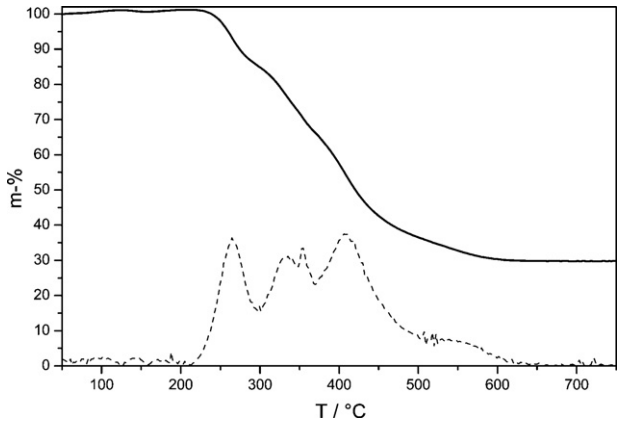

Fig. 1. Thermogravimetric analysis for the FAA membrane in OH^- form.

performed. Results from the thermogravimetric heating of the FAA-2 membrane in its dried OH^- form is shown in Fig. 1. The thermal decomposition of the membrane shows similar trend to many PEM materials [31–33]: it begins at 210 °C and shows steady loss of weight indicating that the thermal properties of the membrane are appropriate for MEA preparation and for fuel cell use.

Thermograms of the FAA-2 membranes in water, methanol and in water methanol mixtures are shown in Fig. 2. The endothermic peaks in the scans correspond to the melting of ice in the samples. The FAA-2 membranes in water and in water–methanol solutions show a two-step melting of the water inside the membranes (Fig. 2). For water and water methanol mixtures the first broad endotherm takes place between −50 °C and −18 °C and the second between −15 °C and −1 °C. With increasing methanol concentration the endotherms are shifted to lower temperatures and for the membrane immersed in pure methanol no endotherm is observed. This behaviour indicates that water in the membranes is most likely crystallised in different environments inside the membrane. These could either be differently sized water filled ionic clusters as water melting temperature is largely dependent on the pore size or due to different chemical nature of the water environments in the membrane. Often water interacting with ionic groups in such membranes is classified as "non-freezing" water residing at closest hydration layer giving no calorimetric signal and "freezable bound" water which shows a melting endotherm at lower temperatures typically broadening the signal from freezable water [34]. The amount of freezable water has been calculated based on the integration of the melting endotherms and presented in Table 2.

The water content in the membranes decreases with increasing methanol concentration, but the amount of freezable water is not

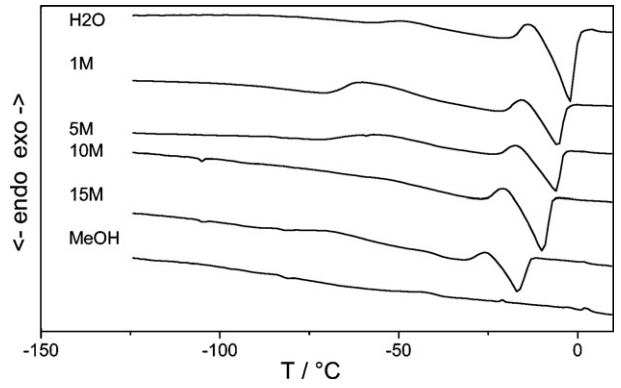

Fig. 2. Calorimetric scans of the FAA-2 membranes at different methanol concentrations.

Table 2
Liquid uptakes, heats of fusion of water (ΔH_f), freezable water content (W_f) and corresponding number of water molecules (λ) per fixed charge of the membranes.

cMeOH (mol l^{-1})	ΔH_f (J g^{-1})[a]	ΔH_f (J g^{-1})[b]	W_f (%)[b]
FuMA-Tech FAA-2			
0	52.7	85.7	25.7
1	37.8	71.8	21.5
5	31.6	61.1	18.3
10	40.0	97.1	29.1
15	21.5	70.5	21.1
24.75	–	–	–
Nafion 115			
0	52.8	154.6	46.3
1	46.0	137.9	41.3
5	46.7	139.8	41.9
10	45.3	166.4	49.9
15	14.5	68.4	20.5
24.75	–	–	–

[a] Enthalpy change for membrane and liquid.
[b] Normallised to the freezing water in the membrane.

as significantly affected and in the case of 10 mol dm^{-3} methanol it even exceeds the enthalpy of melting in pure water. The effect may be explained by the lack of freezing of methanol in the samples, as the supercooled methanol may replace the water in the solvation of the ionic groups (bound water/methanol) and increase the fraction of freezable water [35]. The fact that no melting peak corresponding to methanol dihydrate is observed in the melting of binary methanol–water mixtures supports this conclusion. Further, the interactions of water and methanol in the membranes were studied by NMR. The ^{1}H NMR spectra of different water and water–methanol treated FAA-2 samples are shown in Fig. 3.

From Fig. 3 it can be seen that a broad signal around 2–5 ppm is observed for the immersed membranes, most likely originating from the OH^- protons in the membrane. For closer inspection of the hydroxyl ion diffusion by this method we tried to determine

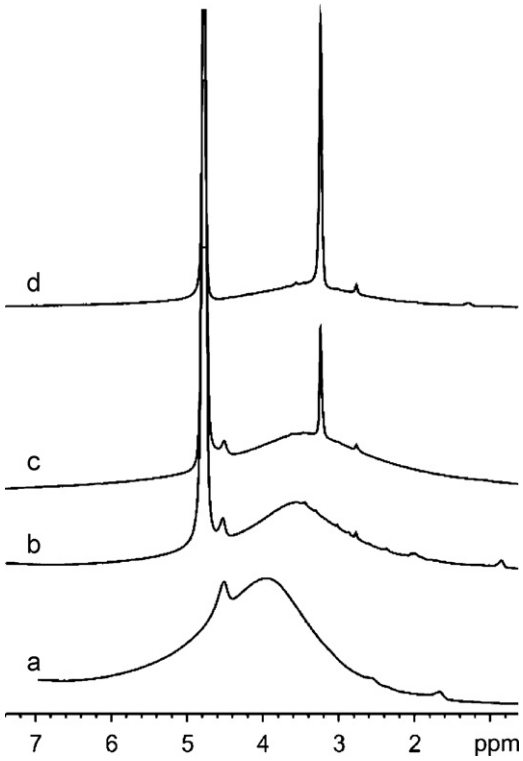

Fig. 3. ^{1}H NMR spectra of (a) 100% relative humidity equilibrated sample, (b) sample immersed in D_2O, (c) sample immersed in 5 mol dm^{-3} CD_3OD in D_2O solution and (d) sample immersed in CD_3OD.

Table 3
Self-diffusion coefficients of water in the FAA-2 membrane with different solvent compositions.

cMeOH (mol dm^{-3})	$D \times 10^{10}$ (m^2 s^{-1})
100% RH	1.5
0	5.1
1	5.3
5	7.0
10	4.2
15	2.8
24.72	–

the diffusion coefficient by the pulsed field gradient NMR (PFG-NMR) [36]. However, the T2 relaxation time of this signal is too short to allow measurement of diffusion coefficient by this method – the signal is fully attenuated already at very short delay times or low gradient strengths. However the signal at 4.6 ppm, assigned to the bound water in the membrane as it is absent from the sample immersed in CD_3OD, is measurable using the PFG–NMR method. The diffusion coefficients determined by this method are shown in Table 3.

The self-diffusion coefficients around $1.5–7 \times 10^{-10}$ m^2 s^{-1} are comparable to those found for the Nafion 117 and PVDF-g-PSSA proton exchange membranes with the same method [37,38]. Compared with the Nafion membranes though, the liquid uptake is much higher in the present membranes, and the lower self-diffusion coefficients for water indicate a tighter and more homogeneous membrane structure compared with the established cluster model in the Nafion membranes. This conclusion is further supported by the observed short relaxation times for the hydroxyls/bound water, which indicate more intimate contacts with the membrane material. The diffusion coefficient of hydroxyls in this membrane obtained by applying the Nernst–Einstein equation (1) [37,39] is around 5×10^{-12} m^2 s^{-1} in pure water and in the methanol solutions.

Thermograms of the Nafion 115 membranes in water, methanol and in water–methanol mixtures are shown in Fig. 4. Unlike the FAA-2 membrane, only one endothermic transition is seen. For water the melting transition has its maximum very close to 0 °C and increasing the methanol content shifts the melting point to lower temperatures, until no transition is seen for the sample in methanol. With increasing methanol concentration the melting enthalpy does not change significantly up to methanol concentration of 10 mol dm^{-3} as shown in Fig. 4 and Table 2. The data for Nafion 115 in water and methanol resembles the melting behaviour reported in the literature for Nafion 117 [35].

The observed differences in the melting behaviour of the two membranes originate from the different chemical and physical compositions of the membranes. In the Nafion membranes water is thought to be residing in a clustered structure in pores of diameter of ~4 nm connecting with narrower diameter channels, both having an ionic surface consisting of acidic SO_3^- groups. Due to the interaction with the ionic groups and polymer matrix, not all the water is capable to crystallize. The measurable water melting is shifted to lower temperatures due to the small size of the water residing in the pores and channels, as commonly observed for water in controlled pore size solids [40]. With the addition of methanol the melting point shifts to lower temperatures and Nafion swells as shown by the liquid uptake measurements (Table 1). However, this does not necessarily mean that the structure is changed significantly, as similar melting point depression is readily observed for binary water–methanol mixtures with increasing methanol concentration.

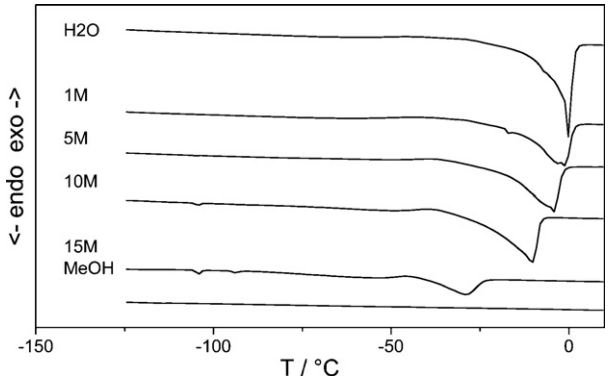

Fig. 4. Calorimetric scans of the Nafion 115 membranes.

Based on DSC measurements for the FAA-2 membranes the freezable water content is much lower than for Nafion 115 throughout the studied concentrations although the solvent uptake is higher. Notably also the melting behavior is significantly different with the two melting peaks (Fig. 2) and melting point depression is less pronounced than for Nafion with increasing methanol concentration. This implies that both the interaction of water with the FAA-2 membrane differs from that of Nafion and, additionally that the membrane structure may contain different water environments, as shown by the thermal behaviour. On the basis of these results the structure of the FAA-2 membrane resembles closely membranes with more homogeneous distribution of ionic groups and solvent, such as irradiation grafted poly(vinylidene fluoride) (PVDF) membranes [36].

Methanol crossover was studied in a diffusion cell because in fuel cell tests the crossover phenomenon is difficult to separate from other effects. The crossover chambers were stabilised to the same temperature, 30 °C, as used in the fuel cell experiments. The calculated methanol permeabilities are independent on the initial methanol concentration and are 3.1×10^{-6} cm^2 s^{-1} and 0.5×10^{-6} cm^2 s^{-1} for Nafion 115 and FAA-2, respectively. This indicates that methanol permeability through the alkaline FAA-2 membrane is six times lower than through the PEM. The values obtained for the AEM are of the same magnitude as similar materials reported at low temperatures [16,23,24,41–43]. In an operating fuel cell transport of methanol is expected to be lower because electro-osmotic drag counteracts diffusion.

3.2. In situ fuel cell studies

In addition to the ex situ studies the performance of the FAA-2 membrane has been studied also in a fuel cell as a part of the membrane electrode assembly (MEA). Prior to use the MEA has been heat pressed at 80 °C, which has proven to be essential for the ADMFC operation [44]. After stabilization overnight in the fuel cell, the performance of the alkaline DMFC with different water–methanol mixtures has been measured and illustrated in Fig. 5. Fig. 5 indicates that both the open circuit voltage (OCV) and the current density maximum depend strongly on the fuel concentration used. The maximum OCV for this cell (580 mV) is obtained with 1 mol dm^{-3} methanol and is higher than the corresponding value measured for the PEM DMFC (520 mV) at the same conditions [45]. This is most likely due to the low methanol permeability though AEM compared to the Nafion PEM leading to the increased OCV of the whole cell. This value is also in agreement with the one obtained with other AEM materials and aqueous methanol fuel by Varcoe et al. at 50 °C [16] and Bunazawa and Yamazaki at 80 °C [46]. However, when comparing these values to the results of the groups using KOH in their anode fuels deliberation is advised because in alkaline solution methanol is partly dissociated to negatively charged methoxy ions influencing both to the adsorption on the electrocatalyst and the crossover mechanisms. When more concentrated methanol

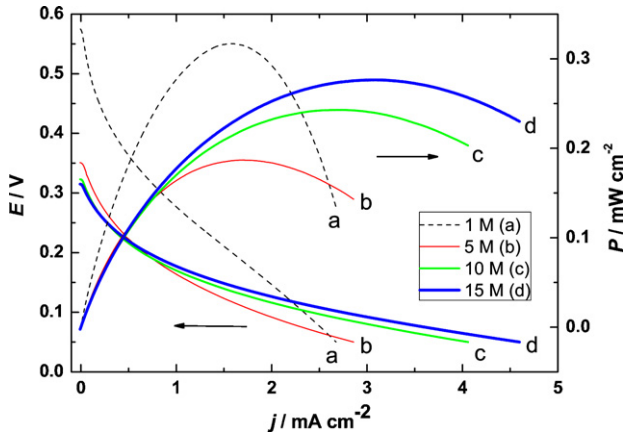

Fig. 5. Polarization and power density curves for the alkaline DMFC as a function of aqueous methanol concentrations.

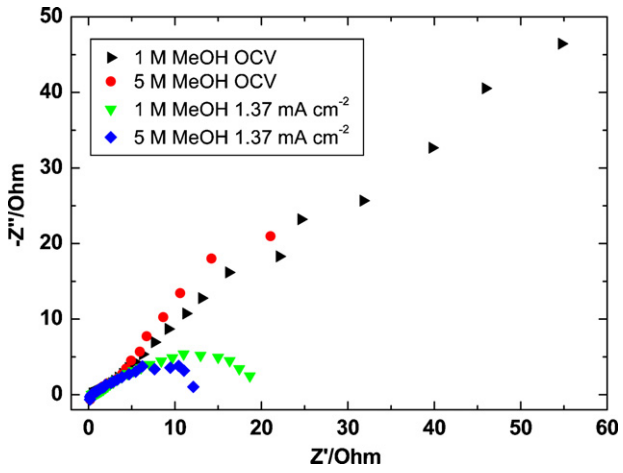

Fig. 6. The electrochemical impedance spectra of the alkaline DMFC obtained with constant current of 0 and 1.37 mA cm^{-2} is represented as Nyquist plot for 1 and 5 mol dm^{-3} methanol solutions.

solutions are used, the OCV of the cell decreases dramatically. This is undoubtedly due to the increasing crossover of methanol through the thin FAA membrane and the membrane swelling (Table 1). These findings are in contrast with the studies made by Yu et al. and Kim et al. who have reported nearly constant OCV for methanol concentrations between 1 and 4 or 3 and 10 mol dm^{-3}, respectively [9,15]. However, both of these groups have used 1 mol dm^{-3} NaOH or KOH added to the anode fuel and obtained clearly higher OCV values around 650–780 mV indicating different electrode processes induced by the alkaline fuel.

In PEM DMFCs the current densities decrease with the use of more concentrated methanol solutions [47,48] due to the severe methanol crossover that interferes cathode reactions and therefore, 2 mol dm^{-3} anode fuel has been found to be the optimum [49]. This implies that a vast amount of water is needed to dilute the fuel even if it is not needed for the anode reaction stoichiometry. This excess water increases the weight of the fuel cell system and complicates the use of DMFCs in mobile applications. On the contrary, with an AEM DMFC the maximum current density is obtained with a nearly pure methanol solution (Fig. 5) which from the point of view of the application is preferable. These results correspond to the findings of Kim et al. who have also noticed higher current densities with higher methanol concentrations [15].

With the 1 mol dm^{-3} fuel the power density maximum of 0.3 mW cm^{-2} is obtained at low current densities. This value is somewhat lower then 1.17 mW cm^{-2} obtained by Varcoe et al [16] with their MEA at 50 °C. However, fuel cell operating at higher temperature and with 4 times higher catalyst loading (4 mg cm^{-2}) can be assumed to have a better performance and the results are not directly comparable to those obtained with the FAA-2 membrane. MEA optimization will also increase the maximum power density; however, it is a topic of a further study. When the concentration is increased to 5 mol dm^{-3} the liquid uptake further increased (Table 1) that allows more methanol to diffuse through the MEA resulting as a performance lost. However, with more concentrated anode fuels some structural change in the membrane matrix that has been also observed with the liquid uptake (Table 1) occurs. Therefore, the power density maximum is shifted to higher currents with the values of 0.15–0.25 mW cm^{-2}. These results indicate that changes in the membrane morphology would seem to effect positively to fuel cell performance. Overall, these power densities are low compared to the PEM DMFC with Nafion membrane due to the lower conductivity of the OH^- ions in the AEM material (Table 1).

After the experiments with aqueous methanol solutions, KOH has been added to the methanol fuel (the concentrations of both components being 1 mol dm^{-3}) to demonstrate the effect of added alkaline solution to the OCV and current density of the cell. With this fuel the OCV increased to 660 mV indicating that in the presence of KOH the cell voltage is at least 50 mV higher. This is associated to the modified reaction kinetics due to the dissociation of methanol molecule at high pH and to the interactions of OH^- ions with the catalyst surface. A similar effect has been seen in the two other studies done with an alkaline anode fuel [9,15]. The pK_a value for methanol is 15.5 [50] indicating that in 1 mol dm^{-3} KOH or NaOH solution (pH 14) methanol is partly dissociated to methoxy (CH_3O^-) ion. The adsorption and the crossover of methoxy ion diverges from that of methanol and therefore, these results cannot be directly compared. Furthermore, after the addition of the base in the cell an 18 times higher current density and a 20 times higher power density maximum has been obtained compared to non alkaline fuels. However, if alkaline anode solution is used, the disadvantages of the traditional alkaline fuel cells are faced and all the cell components need to be selected bearing in mind the component corrosion at high pH.

In addition to the polarisation studies also electrochemical impedance spectra (EIS) has been measured. The spectra are measured with galvanostatic mode to facilitate the evaluation of charge transfer that is inversely proportional to the exchange current density. Two current ranges have been selected: at the OCV of the cell where the current remains zero and at a 1.37 mA cm^{-2} current density corresponding to a potential region of 0.15–0.25 V that could be used in fuel cell applications. The typical Nyquist plots for both currents are presented in Fig. 6 for 1 and 5 mol dm^{-3} methanol solutions. In the hydrogen/oxygen PEMFC the oxygen reduction is sluggish compared to the hydrogen oxidation at the anode and therefore losses are higher at the cathode. It is widely agreed that at low temperatures methanol oxidation is slower than oxygen reduction and therefore, in the ADMFC the limiting reaction takes place at the anode. Consequently, the losses at the cathode are not notable when enough water is available in the cell for oxygen reduction.

With close examination of the Nyquist plots (Fig. 6) two semi circles which partly overlap can be seen. The first semi circle appearing at high frequencies has a very small diameter and is similar for all concentrations studied. However, the second semi circle at lower frequencies is clearly visible and curves towards the Z'-axis when current is drawn due to decrease in over potential and in reaction resistance (R_{ads}) [51]. Ohmic resistances of the membrane, electrodes and their interfaces are included into the resistor R_{m+e+if}. This resistance can be estimated as the value obtained from the intersection of the real axis and the first semicircle in Fig. 6. For all of the experiments, the same cell assembly is used and therefore,

Table 4
The ohmic resistance of the MEA obtained with EIS.

CMeOH (mol dm^{-3})	I (mA cm^{-2})	R_{m+e+if} (Ω)
1	0	0.44
5	0	0.39
10	0	0.49
15	0	0.52
1	1.37	0.49
5	1.37	0.39
10	1.37	0.48
15	1.37	2.2

only the thickness of the MEA changes with the methanol concentration. Table 4 illustrates that this total resistance is independent of the methanol concentration at the three lowest concentrations indicating that the increasing liquid uptake presented in Table 1 has no effect on the cell resistance. However, when very concentrated methanol solutions are used (15 mol dm^{-3}) not enough water is present in the cell and the resistance increases.

4. Conclusions

In this work a new fumasep FAA-2 membrane is introduced and successfully used in an alkaline DMFC as a part of the membrane electrode assembly. In addition, a set of ex and in situ methods to study the suitability of this anion exchange membrane is presented. The results indicate that the membrane is very thin; however, it swells with methanol solutions and doubles its size in pure methanol. The conductivity is in a same range than with other AEM materials at room temperature due to the slow mobility of the OH^- ion. The analysis with calorimetric and NMR experiments implies that the structure of the FAA-2 membrane differs from the clustered structure of Nafion and resembles more with membranes having homogeneous distribution of ionic groups and solvent throughout the membrane. This difference in structure leads to different thermal behaviour of the embedded solvent, lower self-diffusion coefficients of water and results in lower conductivity Fuel cell tests with FAA-2 AEM have been performed successfully and the highest power density has been obtained with 1 mol dm^{-3} methanol fuel. However, the results imply that even highly concentrated fuels (up to 10 mol dm^{-3}) can be used to produce higher current densities in application due to lower methanol crossover. This would evidently facilitate the water management in the cell and reduce the cost of the whole fuel cell system. Electrochemical impedance measurements (EIS) have shown to be a powerful tool for MEA characterization and can provide information for membrane development. These measurements confirm that liquid water is vital for the cathode reaction of the ADMFC. In light of these results AEM materials have shown their advantages compared to the conventional PEM. After further development of these new materials and a suitable catalyst, commercialization of the alkaline DMFC can be reached.

Acknowledgment

The Academy of Finland is acknowledged for financial support.

References

[1] A.V. Tripkovic, K.D. Popovic, B.N. Grgur, B. Blizanac, P.N. Ross, N.M. Markovic, Electrochim. Acta 47 (2002) 3707–3714.
[2] Q. Yi, W. Huang, J. Zhang, X. Liu, L. Li, Catal. Commun. 9 (2008) 2053–2058.
[3] V.A. Kazakov, V.N. Titova, A.A. Yavich, N.V. Petrova, M.R. Tarasevich, Russ. J. Electrochem. 40 (2004) 679–683.
[4] V. Raghuveer, K.R. Thampi, N. Xanthopoulos, H.J. Mathieu, B. Viswanathan, Solid State Ionics 140 (2001) 263–274.
[5] R.N. Singh, A. Singh, D. Mishra, A.P. Chartier, J. Power Sources 185 (2008) 776–783.
[6] A. Verma, A.K. Jha, S. Basu, J. Power Sources 141 (2005) 30–34.
[7] L. Jorissen, J. Power Sources 155 (2006) 23–32.
[8] M. De Konick, S.-C. Poirier, B. Marsan, J. Electrochem. Soc. 154 (2007) A381–A389.
[9] E.H. Yu, K. Scott, J. Power Sources 137 (2004) 248–256.
[10] K. Scott, E. Yu, G. Vlachogiannopoulos, M. Shivare, N. Duteanu, J. Power Sources 175 (2008) 452–457.
[11] H. Bunazawa, Y. Yamazaki, J. Power Sources 182 (2008) 48–51.
[12] Y.S. Li, T.S. Zhao, Z.X. Liang, J. Power Sources 187 (2009) 387–392.
[13] J. Kim, T. Momma, T. Osaka, J. Power Sources 189 (2009) 999–1002.
[14] C. Coutanceau, L. Demarconnay, C. Lamy, J.-M. Leger, J. Power Sources 156 (2006) 14–19.
[15] J.-H. Kim, H.-K. Kim, K.-T. Hwang, J.-Y. Lee, Int. J. Hydrogen Energy 35 (2010) 768–773.
[16] J.R. Varcoe, R.C.T. Slade, E.L.H. Yee, S.D. Poynton, D.J. Driscoll, J. Power Sources 173 (2007) 194–199.
[17] J.R. Varcoe, S.D. Poynton, R.C.T. Slade, in: W. Vielstich, H. Yokokawa, H.A. Gasteiger (Eds.), Hand book of Fuel Cells, vol. 5, John Wiley & Sons, London, 2009, pp. 322–333 (Chapter 21).
[18] E. Agel, J. Bouet, J.F. Fauvarque, J. Power Sources 101 (2001) 267–274.
[19] J.R. Varcoe, R.C.T. Slade, Fuel Cells 5 (2005) 187–200.
[20] A. Wexler, in: D.R. Lide (Ed.), CRC Handbook of Chemistry and Physics, 73rd ed., 1992, pp. 15–20, London.
[21] R.F. Silva, S. Passerini, A. Pozio, Electrochim. Acta 50 (2005) 2639–2645.
[22] P. Dimitrova, K.A. Friedrich, B. Vogt, U. Stimming, J. Electroanal. Chem. 532 (2002) 75–83.
[23] G. Xie, T. Okada, Electrochim. Acta 41 (1996) 1569–1571.
[24] X. Ren, W. Henderson, S. Gottesfeld, J. Electrochem. Soc. 144 (1997) L267–L270.
[25] T. Kallio, K. Kisko, K. Kontturi, R. Serimaa, F. Sundholm, G. Sundholm, Fuel Cells 4 (2004) 328–336.
[26] Z. Wu, G. Sun, W. Jin, H. Hou, S. Wang, J. Membr. Sci. 325 (2008) 376–382.
[27] Y. Xiong, Q.L. Liu, Q.H. Zeng, J. Power Sources 193 (2009) 541–546.
[28] Y. Xiong, J. Fang, Q.H. Zeng, Q.L. Liu, J. Membr. Sci. 311 (2008) 319–325.
[29] C.-C. Yang, S.-J. Chiu, K.-T. Lee, W.-C. Chien, C.-T. Lin, C.-A. Huang, J. Power Sources 184 (2008) 44–51.
[30] R.F. Silva, M. De Francesco, A. Pozio, J. Power Sources 134 (2004) 18–26.
[31] N. Walsby, F. Sundholm, T. Kallio, G. Sundholm, J. Polym. Sci. Part A: Polym. Chem. 39 (2001) 3008–3017.
[32] Q.H. Zeng, Q.L. Liu, I. Broadwell, A.M. Zhu, Y. Xiong, X.P. Tu, J. Membr. Sci. 349 (2010) 237–243.
[33] S. Zhang, T. Xu, C. Wu, J. Membr. Sci. 269 (2006) 142–151.
[34] T.L. Kalapos, B. Decker, H.A. Every, H. Ghassemi, T.A. Zawodzinski Jr., J. Power Sources 172 (2007) 14–19.
[35] R.H. Corti, F. Nores-Pondal, M.J. Pilar Buera, J. Power Sources 161 (2006) 799–805.
[36] S. Hietala, S.L. Maunu, F. Sundholm, T. Lehtinen, G. Sundholm, J. Polym. Sci. Part B: Polym. Phys. 37 (1999) 2893–2900.
[37] N. Walsby, S. Hietala, S.L. Maunu, F. Sundholm, T. Kallio, G. Sundholm, J. Appl. Polym. Sci. 86 (2002) 33–42.
[38] S. Hietala, S.L. Maunu, F. Sundholm, J. Polym. Sci. Polym. Phys. 38 (2000) 3277–3284.
[39] T.A. Zawodzinski, M. Neeman, L.O. Sillerud, S. Gottesfeld, J. Phys. Chem. 95 (1991) 6040–6044.
[40] G.K. Rennie, J. Clifford, J. Chem. Soc. Faraday Trans. 73 (1977) 680–689.
[41] H. Hou, G. Sun, R. He, B. Sun, W. Jin, H. Liu, Q. Xin, Int. J. Hydrogen Energy 33 (2008) 7172–7176.
[42] L. Li, Y.X. Wang, J. Membr. Sci. 262 (2005) 1–4.
[43] L. Wu, T. Xu, D. Wu, X. Zheng, J. Membr. Sci. 310 (2008) 577–585.
[44] C.-M. Lai, J.-C. Lin, K.-L. Hsueh, C.-P. Hwang, K.-C. Tsay, L.-D. Tsai, Y.-M. Peng, Int. J. Hydrogen Energy 32 (2007) 4381–4388.
[45] A. Santasalo, T. Kallio, K. Kontturi, Platinum Met. Rev. 53 (2009) 58–66.
[46] H. Bunazawa, Y. Yamazaki, J. Power Sources 190 (2009) 210–215.
[47] S.-H. Yang, C.-Y. Chen, W.-J. Wang, J. Power Sources 195 (2010) 2319–2330.
[48] K. Lee, J.-D. Nam, J. Power Sources 157 (2006) 201–206.
[49] S. Song, W. Zhou, Z. Liang, R. Cai, G. Sun, Q. Xin, V. Stergiopoulos, P. Tsiakaras, Appl. Catal. B: Environ. 55 (2005) 65–72.
[50] J. Clayden, N. Greeves, S. Warren, P. Wothers, Organic Chemistry, Oxford University Press, New York, 2001.
[51] C.A. Schiller, F. Richter, E. Gülzow, N. Wagner, Phys. Chem. Chem. Phys. 3 (2001) 2113–2116.